

# Linear stability of finite-amplitude capillary waves on water of infinite depth

Roxana Tiron<sup>1</sup> and Wooyoung Choi<sup>1,2†</sup>

<sup>1</sup> Department of Ocean Systems Engineering, Korea Advanced Institute of Science and Technology,  
Daejeon, 305-701, Korea

<sup>2</sup> Department of Mathematical Sciences, New Jersey Institute of Technology,  
Newark, NJ 07102-1982, USA

(Received 15 May 2011; revised 28 November 2011; accepted 25 January 2012;  
first published online 6 March 2012)

We study the linear stability of the exact deep-water capillary wave solution of Crapper (*J. Fluid Mech.*, vol. 2, 1957, pp. 532–540) subject to two-dimensional perturbations (both subharmonic and superharmonic). By linearizing a set of exact one-dimensional non-local evolution equations, a stability analysis is performed with the aid of Floquet theory. To validate our results, the exact evolution equations are integrated numerically in time and the numerical solutions are compared with the time evolution of linear normal modes. For superharmonic perturbations, contrary to Hogan (*J. Fluid Mech.*, vol. 190, 1988, pp. 165–177), who detected two bubbles of instability for intermediate amplitudes, our results indicate that Crapper's capillary waves are linearly stable to superharmonic disturbances for all wave amplitudes. For subharmonic perturbations, it is found that Crapper's capillary waves are unstable, and our results generalize to the highly nonlinear regime the analysis for small amplitudes presented by Chen & Saffman (*Stud. Appl. Maths*, vol. 72, 1985, pp. 125–147).

**Key words:** capillary waves

## 1. Introduction

The stability of periodic gravity and gravity–capillary waves has been the subject of extensive research. For comprehensive reviews, see, for instance, Hammack & Henderson (1993) and Dias & Kharif (1999).

Under the weakly nonlinear assumption, Benjamin & Feir (1967) were the first to present conclusive analytical and experimental evidence that nonlinear wave trains of gravity waves on deep water are unstable to long-wavelength perturbations. Soon thereafter, Zakharov (1968) derived the cubic nonlinear Schrödinger equation and retrieved the same instability result. Benney & Roskes (1969) extended Zakharov's result to water of finite depth, while the extension to gravity–capillary waves is due to Djordjevic & Redekopp (1977) and Hogan (1985) for water of finite and infinite depth, respectively.

At the same time, numerical studies of linear stability of periodic gravity waves of finite amplitude have been carried out to compute the full spectrum and the corresponding normal modes. Using a hodograph transformation, where the dependent

† Email address for correspondence: [wychoi@njit.edu](mailto:wychoi@njit.edu)

and independent variables are interchanged so that the spatial coordinates are functions of the stream function and the velocity potential in the frame travelling with the wave, Longuet-Higgins (1978a,b) studied the stability of finite-amplitude gravity waves on deep water to both subharmonic and superharmonic perturbations. However, he considered only two-dimensional perturbations. The spectrum calculations for three-dimensional perturbations were performed by McLean *et al.* (1981) and McLean (1982a) for gravity waves and by Zhang & Melville (1987) for gravity–capillary waves. These results were further extended to finite-depth water by McLean (1982b), Nicholls (2009) and Deconinck & Oliveras (2011).

While one is required to compute numerically periodic progressive wave solutions to study stability of finite-amplitude gravity or gravity–capillary waves, exact analytic solutions of the Euler equations have been known for pure capillary waves. The closed-form solutions obtained ingeniously by Crapper (1957) are of particular interest owing to their highly nonlinear features. The maximum wave steepness measured as the ratio of the wave height to the wavelength ( $H/\lambda$ ) is approximately 0.73, which is much greater than that for gravity waves (approximately 0.14). Furthermore, for sufficiently large amplitudes, the wave profile becomes multivalued and a trapped bubble is formed at the trough of the wave. We remark that Vanden-Broeck & Keller (1980) have found numerically a new class of periodic solutions that can attain greater steepness than Crapper’s solution.

Chen & Saffman (1985) were the first to study the stability of Crapper’s capillary wave solution subject to subharmonic perturbations. Since they were interested in stability characteristics under three-dimensional perturbations, the hodograph transformation based on conformal mapping is no longer applicable. Therefore, rather than using Crapper’s solution written parametrically in terms of the stream function and the velocity potential, the analysis was performed by expanding Crapper’s solution in Fourier series in physical space. Unfortunately, owing to the highly nonlinear nature of pure capillary waves mentioned previously, Chen & Saffman (1985) found that the convergence of the Fourier series becomes very slow even for wave amplitudes considerably smaller than the maximum value. Therefore, Chen & Saffman (1985) have shown that capillary waves are unstable to subharmonic perturbations, but obtained reliable results only for wave steepness up to, roughly,  $H/\lambda = 0.12$ .

Hogan (1988) noticed this amplitude limitation and, using a similar method to Longuet-Higgins (1978a,b), performed a two-dimensional stability analysis, covering the entire range of amplitudes from zero to the maximum value. He considered only the case of superharmonic perturbations and detected two bubbles of instability for intermediate wave amplitudes. Hogan (1988) further remarked that his result is consistent with a necessary condition for instability that MacKay & Saffman (1986) found in terms of eigenvalue signature representing physically the energy in a frame of reference moving with the wave (see (3.5) for the mathematical definition of eigenvalue signature). In relatively simple terms, the condition states that instability could occur only when two eigenvalues of opposite signature collide as the wave amplitude increases from zero. (A more accurate statement is given in § 3.) After re-examining the signatures of the two pairs of eigenvalues that were found to collide by Hogan (1988), it is noticed that they have the same signature and, therefore, the conclusion of Hogan (1988) on the emergence of unstable modes is apparently inaccurate.

With these observations in mind, in this paper, we aim to verify the result for superharmonic perturbations reported by Hogan (1988) and extend the weakly nonlinear result of Chen & Saffman (1985) for subharmonic disturbances to the highly

nonlinear regime. To achieve this, we use a system of exact one-dimensional, non-local evolution equations derived by Ovsjannikov (1974) and Dyachenko, Zakharov & Kuznetsov (1996), which is an alternative and markedly more concise approach to that used by Longuet-Higgins (1978a,b) and Hogan (1988). The system of integro-differential equations obtained using a time-dependent conformal mapping technique to map the free surface onto a flat surface satisfies Crapper's solution in the steady limit and, therefore, the stability analysis can be carried out by linearizing the system about Crapper's solution in a straightforward manner. In addition, the system can be integrated in time using, for example, an accurate pseudospectral method (Choi & Camassa 1999; Li, Hyman & Choi 2004), and thus the exact time evolution of perturbed capillary waves of finite amplitude can be studied numerically without adopting an alternative formulation such as a boundary integral formulation.

The paper is structured as follows. In § 2, we introduce the exact evolution equations and formulate the eigenvalue problem by linearizing the equations around the exact solution of Crapper (1957). In § 3, we look at the spectrum in the limit of zero amplitude and discuss eigenvalue signature. In particular, we focus on the necessary condition for loss of spectral stability that MacKay & Saffman (1986) found. With the numerical implementation of the eigenvalue problem described in § 4, we present our findings for both superharmonic and subharmonic perturbations in §§ 5.1 and 5.2, respectively. To validate our results, we present comparisons between the time evolution of the normal modes predicted by the linear stability theory and numerical solutions of the exact evolution equations. We summarize our conclusions in § 6.

## 2. Perturbation analysis

### 2.1. Exact evolution equations and periodic wave solution

By using a conformal mapping technique, it has been shown (Ovsjannikov 1974; Dyachenko *et al.* 1996; Choi & Camassa 1999) that the kinematic and dynamic free-surface boundary conditions can be reduced to a closed system of exact evolution equations for the surface elevation  $y(\xi, t)$  and the velocity potential at the free surface  $\phi(\xi, t)$  parametrized by a real parameter  $\xi$ :

$$y_t = y_\xi \mathcal{H} \left[ \frac{\psi_\xi}{J} \right] - x_\xi \frac{\psi_\xi}{J}, \quad (2.1)$$

$$\phi_t = -\frac{1}{2J} (\phi_\xi^2 - \psi_\xi^2) + \phi_\xi \mathcal{H} \left[ \frac{\psi_\xi}{J} \right] + \frac{T x_\xi y_{\xi\xi}}{\rho J^{3/2}} - \frac{y_\xi x_{\xi\xi}}{J^{3/2}}, \quad (2.2)$$

where the subscript denotes differentiation,  $T$  is the surface tension, and  $\mathcal{H}$  is the Hilbert transform given by

$$\mathcal{H}[y] = \frac{1}{\pi} \int_{-\infty}^{\infty} \frac{y(\xi', t)}{\xi' - \xi} d\xi'. \quad (2.3)$$

In (2.1) and (2.2), the Jacobian  $J$  is defined as

$$J = x_\xi^2 + y_\xi^2, \quad (2.4)$$

and  $x(\xi, t)$  and  $\psi(\xi, t)$  (the horizontal coordinate and the stream function on the surface) are related to  $y$  and  $\phi$  by

$$x_\xi = 1 - \mathcal{H}[y_\xi], \quad (2.5)$$

$$\phi_\xi = -U - \mathcal{H}[\psi_\xi], \quad (2.6)$$

where  $U$  is the velocity of a constant background current.

For a periodic wave solution  $(x, y, \phi, \psi) = (X, Y, \Phi, \Psi)$  in a frame of reference moving with the wave speed  $c$ , the problem becomes steady ( $X_t = Y_t = 0$ ), so that, from (2.1) and (2.6) with  $U = c$ , we have

$$\Psi_\xi = 0, \quad \Phi_\xi = -c. \quad (2.7)$$

Then, from  $\Phi_t = -c^2/2$  to fix the Bernoulli constant, (2.2) can be reduced to

$$\frac{1}{2} \frac{c^2}{X_\xi^2 + Y_\xi^2} = \left( \frac{T}{\rho} \right) \frac{X_\xi Y_{\xi\xi} - Y_\xi X_{\xi\xi}}{(X_\xi^2 + Y_\xi^2)^{3/2}} + \frac{c^2}{2}. \quad (2.8)$$

Then it can be shown that the exact solution of Crapper (1957), given by

$$X = \xi - \frac{2\lambda}{\pi} \frac{A \sin(2\pi\xi/\lambda)}{1 + A^2 + 2A \cos(2\pi\xi/\lambda)}, \quad Y = -\frac{2\lambda}{\pi} \left[ 1 - \frac{1 + A \cos(2\pi\xi/\lambda)}{1 + A^2 + 2A \cos(2\pi\xi/\lambda)} \right], \quad (2.9)$$

satisfies (2.5) and (2.8). In (2.9), the parameter  $A$  can be written in terms of the dimensionless wave height  $h = H/\lambda$ , where  $H$  is the wave height and  $\lambda$  is the wavelength,

$$A = \frac{2}{\pi h} \left[ \sqrt{1 + \frac{\pi^2 h^2}{4}} - 1 \right], \quad (2.10)$$

whereas the phase speed  $c$  is given by

$$c = \sqrt{\frac{2\pi T}{\lambda \rho}} \left( 1 + \frac{\pi^2}{4} h^2 \right)^{-1/4}. \quad (2.11)$$

As shown by Crapper (1957), the maximum amplitude occurs for  $h = 0.73$ , for which a trapped bubble can be observed. Without loss of generality, we assume  $T = \rho = 1$  and  $\lambda = 2\pi$ , using the same conventions as in Chen & Saffman (1985), and study the stability of the one-parameter family solution (2.9) with  $h$  in the range of  $[0, 0.73]$ . This is equivalent to non-dimensionalizing the spatial and temporal variable  $t$  with

$$\lambda_0 = \frac{\lambda}{2\pi}, \quad t_0 = \sqrt{\left( \frac{\lambda}{2\pi} \right)^3 \frac{\rho}{T}}, \quad (2.12)$$

respectively.

## 2.2. Linearization around the periodic wave solution

We linearize equations (2.1), (2.2), (2.5) and (2.6) around the periodic wave solution in a frame of reference moving with the wave. Thus, let

$$x = X + \tilde{x}, \quad y = Y + \tilde{y}, \quad \psi = \Psi + \tilde{\psi}, \quad \phi = \Phi + \tilde{\phi}, \quad (2.13)$$

where the quantities denoted by capital letters correspond to the periodic wave solution and the quantities with a tilde denote small perturbations.

By substituting (2.13) into (2.1), (2.2), (2.5) and (2.6) and retaining only linear terms, we obtain the linearized equations for the evolution of the perturbations:

$$\tilde{y}_t = Y_\xi \mathcal{H} \left[ \frac{\tilde{\psi}_\xi}{J_0} \right] - X_\xi \frac{\tilde{\psi}_\xi}{J_0}, \quad (2.14)$$

$$\tilde{\phi}_t = F\tilde{x}_\xi + G\tilde{y}_\xi + \frac{c}{J_0}\tilde{\phi}_\xi - QY_\xi\tilde{x}_{\xi\xi} + QX_\xi\tilde{y}_{\xi\xi} - c\mathcal{H}\left[\frac{\tilde{\psi}_\xi}{J_0}\right], \quad (2.15)$$

$$\tilde{x}_\xi = -\mathcal{H}[\tilde{y}_\xi], \quad (2.16)$$

$$\tilde{\phi}_\xi = -\mathcal{H}[\tilde{\psi}_\xi], \quad (2.17)$$

where  $J_0 = X_\xi^2 + Y_\xi^2$  denotes the Jacobian corresponding to the periodic solution and

$$\left. \begin{aligned} P(\xi) &= \frac{c^2}{2J_0^2}(3J_0 - 1), & Q(\xi) &= \frac{T}{\rho}J_0^{-3/2}, \\ F(\xi) &= PX_\xi + QY_{\xi\xi}, & G(\xi) &= PY_\xi - QX_{\xi\xi}. \end{aligned} \right\} \quad (2.18)$$

### 2.3. Normal mode decomposition

Floquet theory ensures that the general solution of the system of linear integro-differential equations with periodic coefficients given by (2.14)–(2.17) can be represented as a linear combination of normal modes of the form

$$\tilde{x}(\xi, t) = e^{\sigma t}e^{ip\xi} \sum_{j=-\infty}^{\infty} a_j e^{ij\xi}, \quad \tilde{y}(\xi, t) = e^{\sigma t}e^{ip\xi} \sum_{j=-\infty}^{\infty} b_j e^{ij\xi}, \quad (2.19a)$$

$$\tilde{\phi}(\xi, t) = e^{\sigma t}e^{ip\xi} \sum_{j=-\infty}^{\infty} c_j e^{ij\xi}, \quad \tilde{\psi}(\xi, t) = e^{\sigma t}e^{ip\xi} \sum_{j=-\infty}^{\infty} d_j e^{ij\xi}, \quad (2.19b)$$

where  $p$  is real so that the possibility of exponential growth at  $\xi \rightarrow \pm\infty$  is excluded and  $0 \leq p < 1$  is assumed. When  $p = 0$ , the perturbation has a wavelength of  $2\pi$  or less and is called superharmonic. On the other hand, when  $0 < p < 1$ , the normal mode represents a subharmonic perturbation whose wavelength is greater than  $2\pi$ . In (2.19b),  $\sigma = \sigma_R + i\sigma_I$  denotes the complex eigenvalue. If  $\sigma_R > 0$ ,  $\sigma_R$  denotes the growth rate and the corresponding normal mode is unstable.

Using a normal mode of the form (2.19b) and taking into account that

$$\mathcal{H}[e^{i\alpha\xi}] = i \operatorname{sgn}(\alpha) e^{i\alpha\xi}, \quad (2.20)$$

equations (2.16) and (2.17) lead to the following relations between the sets of coefficients  $a_j$ ,  $b_j$  and  $c_j$ ,  $d_j$ , respectively:

$$a_j = -i \operatorname{sgn}(j+p)b_j, \quad d_j = i \operatorname{sgn}(j+p)c_j. \quad (2.21)$$

Note that, when  $j = 0$  and  $p = 0$ ,  $a_0$  and  $d_0$  cannot be derived from the above relations. This apparent arbitrariness is a consequence of the freedom to choose the origin of the reference system in the horizontal direction. Moreover, these two constants do not enter in (2.14) and (2.15) since these equations contain only derivatives with respect to  $\xi$  of  $x$  and  $\psi$ .

By substituting expansion (2.19b) together with (2.21) in (2.14) and (2.15), we obtain an eigenvalue problem for the complex eigenvalue  $\sigma$  and the coefficients  $b_j$  and  $c_j$ :

$$\sigma \sum_{j=-\infty}^{\infty} e^{i(j+p)\xi} b_j = \sum_{j=-\infty}^{\infty} \alpha_{j,p}(\xi) c_j, \quad (2.22)$$

$$\sigma \sum_{j=-\infty}^{\infty} e^{i(j+p)\xi} c_j = \sum_{j=-\infty}^{\infty} \beta_{j,p}(\xi) b_j + \sum_{j=-\infty}^{\infty} \gamma_{j,p}(\xi) c_j, \quad (2.23)$$

where

$$\alpha_{j,p}(\xi) = |j+p| \left\{ \frac{X_\xi}{J_0} e^{i(j+p)\xi} - Y_\xi \mu_{j,p}(\xi) \right\}, \quad (2.24)$$

$$\mu_{j,p}(\xi) = \mathcal{H} \left[ \frac{e^{i(j+p)\xi}}{J_0} \right], \quad (2.25)$$

$$\beta_{j,p}(\xi) = |j+p| e^{i(j+p)\xi} \{ F + i \operatorname{sgn}(j+p) G - (j+p)[iY_\xi + \operatorname{sgn}(j+p)X_\xi]Q \}, \quad (2.26)$$

$$\gamma_{j,p}(\xi) = c(j+p) \left\{ \frac{i e^{i(j+p)\xi}}{J_0} + \operatorname{sgn}(j+p) \mu_{j,p}(\xi) \right\}. \quad (2.27)$$

#### 2.4. Properties of the spectrum

As remarked in Chen & Saffman (1985), the wavenumber  $p$  can be changed by an integer without changing the eigenmode. Furthermore, if  $\{\sigma, p, b_j, c_j\}$  is an eigenset of the system given by (2.22) and (2.23), then (i)  $\{\sigma^*, -p, b_{-j}^*, c_{-j}^*\}$ , (ii)  $\{-\sigma, -p, b_{-j}, -c_{-j}\}$  and (iii)  $\{-\sigma^*, p, b_{-j}^*, -c_{-j}^*\}$  are also eigensets.

To show that (i) is an eigenset, note that

$$\alpha_{j,p}^* = \alpha_{-j,-p}, \quad \beta_{j,p}^* = \beta_{-j,-p}, \quad \gamma_{j,p}^* = \gamma_{-j,-p}. \quad (2.28)$$

Then, by taking the complex conjugate of (2.22) and (2.23), we obtain

$$\sigma^* \sum_{j=-\infty}^{\infty} e^{-i(j+p)\xi} b_j^* = \sum_{j=-\infty}^{\infty} \alpha_{-j,-p}(\xi) c_j^*, \quad (2.29)$$

$$\sigma^* \sum_{j=-\infty}^{\infty} e^{-i(j+p)\xi} c_j^* = \sum_{j=-\infty}^{\infty} \beta_{-j,-p}(\xi) b_j^* + \sum_{j=-\infty}^{\infty} \gamma_{-j,-p}(\xi) c_j^*. \quad (2.30)$$

The fact that (i) is an eigenset follows after replacing  $j \rightarrow -j$  in these equations.

For eigenset (ii), note that  $X_\xi$  and  $J_0$  are even functions in  $\xi$  whereas  $Y_\xi$  is odd, and also that  $P$ ,  $Q$  and  $F$  are even whereas  $G$  is odd, as can be seen from (2.18). These properties, together with the relation

$$\mathcal{H}[f(\xi)]|_{-\xi} = -\mathcal{H}[f(-\xi)]|_\xi, \quad (2.31)$$

which follows directly from definition (2.3), imply that

$$\alpha_{j,p}(-\xi) = \alpha_{-j,-p}(\xi), \quad \beta_{j,p}(-\xi) = \beta_{-j,-p}(\xi), \quad \gamma_{j,p}(-\xi) = -\gamma_{-j,-p}(\xi). \quad (2.32)$$

Then, by replacing  $\xi$  by  $-\xi$  in (2.22) and (2.23), we obtain

$$\sigma \sum_{j=-\infty}^{\infty} e^{-i(j+p)\xi} b_j = \sum_{j=-\infty}^{\infty} \alpha_{-j,-p}(\xi) c_j, \quad (2.33)$$

$$\sigma \sum_{j=-\infty}^{\infty} e^{-i(j+p)\xi} c_j = \sum_{j=-\infty}^{\infty} \beta_{-j,-p}(\xi) b_j - \sum_{j=-\infty}^{\infty} \gamma_{-j,-p}(\xi) c_j. \quad (2.34)$$

By substituting  $j \rightarrow -j$  in the above equations, it follows that (ii) is also an eigenset. Then, (iii) follows from (i) and (ii).

Finally, the invariance of the spectrum to the change of  $p$  by an integer and the symmetry properties mentioned above imply that the spectrum is antisymmetric with respect to  $p = 1/2$ . In other words, if  $\sigma_R + i\sigma_I$  and  $-\sigma_R + i\sigma_I$  are eigenvalues for  $p \in [0, 1/2]$ , then  $\sigma_R - i\sigma_I$  and  $-\sigma_R - i\sigma_I$  are eigenvalues for  $1-p$ . Thus it suffices to solve the eigenvalue problem for  $p \in [0, 1/2]$ .

### 3. Spectrum in the limit of zero amplitude and Krein signatures

In the limit of  $h = H/\lambda \rightarrow 0$  (equivalently, in the absence of steady periodic waves), the eigenvalue problem given by (2.22) and (2.23) can be reduced to

$$\sigma b_j - |j+p|c_j = 0, \quad [\sigma - 2i(j+p)]c_j - |j+p|(1 - |j+p|)b_j = 0, \quad (3.1)$$

since  $P = c^2$ ,  $Q = 1$ ,  $F = c^2$ ,  $G = 0$ ,  $c = 1$ ,  $\alpha_{j,p} = |j+p| \exp[i(j+p)\xi]$ ,  $\beta_{j,p} = |j+p|(1 - |j+p|) \exp[i(j+p)\xi]$  and  $\gamma_{j,p} = 2i(j+p) \exp[i(j+p)\xi]$ , and its solutions are given by

$$\sigma_m^s = -i[s|p'|^{3/2} - p'], \quad (3.2)$$

where  $p' = p + m$ ,  $m$  is an integer, and  $s = \pm 1$ . Equation (3.2) is nothing but the dispersion relation for capillary waves in a frame travelling with speed 1 (the speed of the periodic solution in the limit  $h \rightarrow 0$ ) since the frequency and phase speed of a normal mode with wavenumber  $p' = p + m$  in the fixed frame are

$$\omega = s|p'|^{3/2} \quad \text{and} \quad c' = \omega/p' = s \operatorname{sgn}(p') |p'|^{1/2}, \quad (3.3)$$

respectively.

MacKay & Saffman (1986) have shown that one could use the Hamiltonian structure of the water wave equations, which was first pointed out by Zakharov (1968), to infer the behaviour of the spectrum for finite-amplitude periodic waves from that for zero-amplitude periodic waves.

Indeed, there is a well-developed theory that describes how the eigenvalues of an equilibrium of a Hamiltonian system can move as parameters change (MacKay 1986). In particular, the second variation of the Hamiltonian associated with a given eigenvalue is a quadratic form, which can be either positive or negative definite, and its sign is called the signature of the eigenvalue, or Krein signature. The signature is preserved as parameters vary as long as eigenvalues do not collide.

Another important result of the theory is the following. If all the eigenvalues of an equilibrium of a Hamiltonian system are purely imaginary and non-zero, then the equilibrium can lose spectral stability as parameters vary only by collision of eigenvalues of opposite signature or by collision of eigenvalues at zero.

The Krein signature of the spectrum at zero wave amplitude has been calculated for the general case of capillary–gravity waves by MacKay & Saffman (1986). They showed that the energy of an infinitesimal disturbance with wavenumber  $p' = p + m$  is given, up to second order, by

$$E = 2\rho\omega(\omega - p')|\zeta_0|^2 = \frac{2\rho}{p'^2}c'(c' - 1)|\zeta_0|^2, \quad (3.4)$$

where  $\zeta_0$  denotes the perturbation amplitude and  $\omega$  is, as before, the frequency in the fixed frame given by (3.3). We note that  $E < 0$  (and thus the Krein signature is  $s_K = -1$ ) for  $0 < c' < 1$ , which corresponds to a perturbation travelling in the same direction as the wave but slower. On the other hand,  $E > 0$  (and thus  $s_K = 1$ ) for  $c' < 0$  or  $c' > 1$ , which correspond to the perturbation travelling either in the opposite direction, or in the same direction as the wave but faster. Alternatively, from (3.2)–(3.4), the signature can be expressed, in terms of  $\sigma_m^s$ , as

$$s_K = \operatorname{sgn}[-s \operatorname{Im}(\sigma_m^s)] = \operatorname{sgn}[-sp' + |p'|^{3/2}]. \quad (3.5)$$

This implies that the signature is negative for  $0 < sp' < 1$ , zero for  $sp' = 0$  or  $sp' = 1$ , and positive otherwise.

For superharmonic perturbations ( $p = 0$ ,  $p' = m$ ), the Krein signature of the eigenvalues at  $h = 0$  is zero for  $sm = 0$  or  $sm = 1$  and positive otherwise. Note that, in this case, zero is an eigenvalue (with multiplicity four). This zero eigenvalue could, in principle, give rise to unstable modes as the amplitude increases. Nonetheless, collisions of non-zero eigenvalues cannot lead to the emergence of unstable modes since they all have the same signature. As discussed in § 5.1, our findings are in agreement with this particular observation and furthermore reveal stability for the entire range of amplitudes from zero to the maximum amplitude.

For subharmonic perturbations ( $p \neq 0$ ), the signature of the eigenvalues in the limit  $h = 0$  is positive except for the pairs  $(m, s) = (-1, -1)$  and  $(0, 1)$  for which the normal modes move to the right in the fixed frame but slower than the carrier wave and hence have negative signature – see figure 1, where we depict the phase speed (in the fixed frame) dependence on the wavenumber  $p$  for several eigenmodes corresponding to  $h = 0$ . This case meets all the requirements of the theory in MacKay (1986) and hence instability can occur only by collisions between branches of opposite signature. As mentioned before, it suffices to look at the range  $p \in (0, 1/2]$ . By examining figure 2, one could expect two such collisions to occur: one between the branches  $(m, s) = (-1, -1)$  and  $(1, 1)$ , and the other between  $(m, s) = (0, 1)$  and  $(0, -1)$  for  $p \in (0, p_0)$  or  $(m, s) = (-2, -1)$  for  $p \in (p_0, 1/2)$  where  $p_0 = 0.31875$  at which the intersection between the branches  $(0, -1)$  and  $(-2, -1)$  occurs. As can be seen in § 5.2, our findings confirm this expectation and moreover reveal that each of these collisions results in the emergence of an unstable branch. However, we note that, as the amplitude increases from  $h = 0$ , two branches of the same signature could cross, but no unstable modes are expected to emerge. Finally we remark that, as noted already by MacKay & Saffman (1986), collision between branches of opposite signature is only a necessary but not a sufficient condition for loss of spectral stability; in fact, the recent work by Nicholls (2009) offers a more restrictive criterion for instability.

#### 4. Numerical implementation

To solve the eigenvalue problem given by (2.22) and (2.23), we recast it as a generalized linear eigenvalue problem as follows. After truncating the infinite series for  $j = -n, \dots, n$ , the unknowns become the eigenvalue  $\sigma$  and two sets of  $2n + 1$  coefficients  $b_j, c_j$ . Next, by denoting

$$\zeta = \{b_{-n}, \dots, b_n, c_{-n}, \dots, c_n\}^T, \quad (4.1)$$

and choosing  $2n + 1$  discretization points within the period of  $2\pi$ ,

$$\xi_k = \frac{2\pi(k-1)}{2n+1} \quad \text{with } k = 1, \dots, 2n+1, \quad (4.2)$$

equations (2.22) and (2.23) can be put in matrix form as

$$\sigma \mathbf{L}\zeta = \mathbf{R}\zeta, \quad (4.3)$$

with  $\mathbf{L}$  and  $\mathbf{R}$  being the  $(4n+2) \times (4n+2)$  matrices

$$\mathbf{L} = \left[ \begin{array}{c|c} \mathbf{E} & \mathbf{O}_{2n+1} \\ \hline \mathbf{O}_{2n+1} & \mathbf{E} \end{array} \right], \quad \mathbf{R} = \left[ \begin{array}{c|c} \mathbf{O}_{2n+1} & \mathbf{A} \\ \hline \mathbf{B} & \mathbf{G} \end{array} \right], \quad (4.4)$$

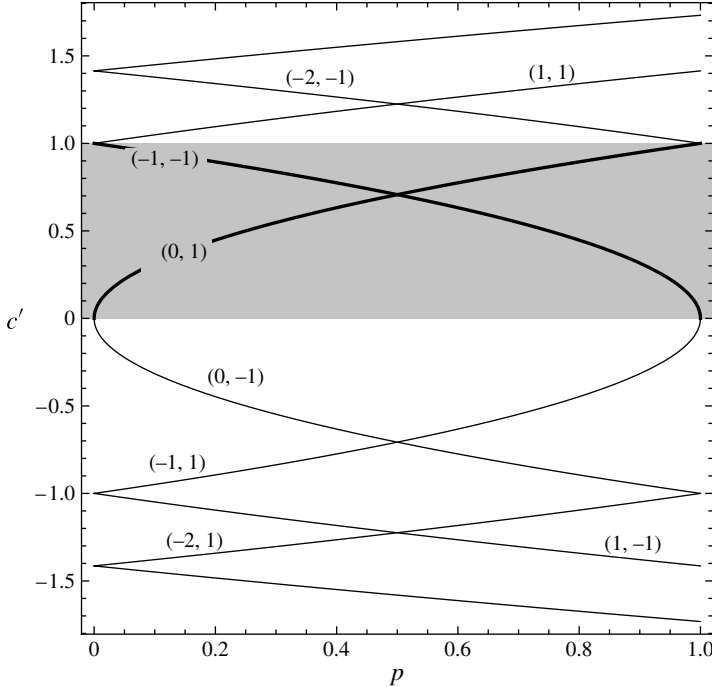


FIGURE 1. Phase speed (in the fixed frame) of the normal modes corresponding to amplitude  $h = 0$ , as a function of the wavenumber  $p$ . The shaded region corresponds to phase speeds between 0 and 1 (the speed of the carrier wave). Normal modes with phase speeds inside this area have negative Krein signatures whereas branches with phase speeds outside it have positive Krein signature.

where  $\mathbf{O}_{2n+1}$  is the  $2n + 1$  square zero matrix, and matrices  $\mathbf{E}$ ,  $\mathbf{A}$ ,  $\mathbf{B}$  and  $\mathbf{G}$  are all square matrices of dimension  $2n + 1$  with components

$$\left. \begin{aligned} \mathbf{E}_{k,l} &= \exp[i(l' + p)\xi_k], & \mathbf{A}_{k,l} &= \alpha_{l',p}(\xi_k), & \mathbf{B}_{k,l} &= \beta_{l',p}(\xi_k), \\ \mathbf{G}_{k,l} &= \gamma_{l',p}(\xi_k), & l' &= l - n - 1, \end{aligned} \right\} \quad (4.5)$$

where the functions  $\alpha$ ,  $\beta$ ,  $\gamma$  are given by (2.24)–(2.27). All the terms defining these functions except the term  $\mu_{j,p}$  are given explicitly in terms of  $\xi$  and, therefore, can be easily evaluated at  $\xi = \xi_k$ . On the other hand,  $\mu_{j,p}$  requires one to evaluate numerically the Hilbert transform of  $\exp[i(j+p)\xi]/J_0$ . This is done by first determining the discrete Fourier transform of  $1/J_0$  via a fast Fourier transform (FFT) and then summing up the resulting linear combination of the Hilbert transforms of exponential functions that are explicitly given by (2.20).

To solve the generalized eigenvalue problem (4.3), we use the QZ algorithm for non-symmetric complex matrices (Garbow 1978) and, for the FFT transform, the FFTPACK package (Swarztrauber 1982). The level of truncation for the Floquet series used was  $n = 128$  and the number of Fourier modes for the Fourier transform of the term  $1/J_0$  was 512.

As discussed in § 3, for superharmonic perturbations ( $p = 0$ ), zero is an eigenvalue with multiplicity 4 when the wave amplitude is zero ( $h = 0$ ). For  $h \neq 0$ , two eigenvalues are identically zero since the  $(n + 1)$ th and  $(3n + 2)$ th columns of matrix

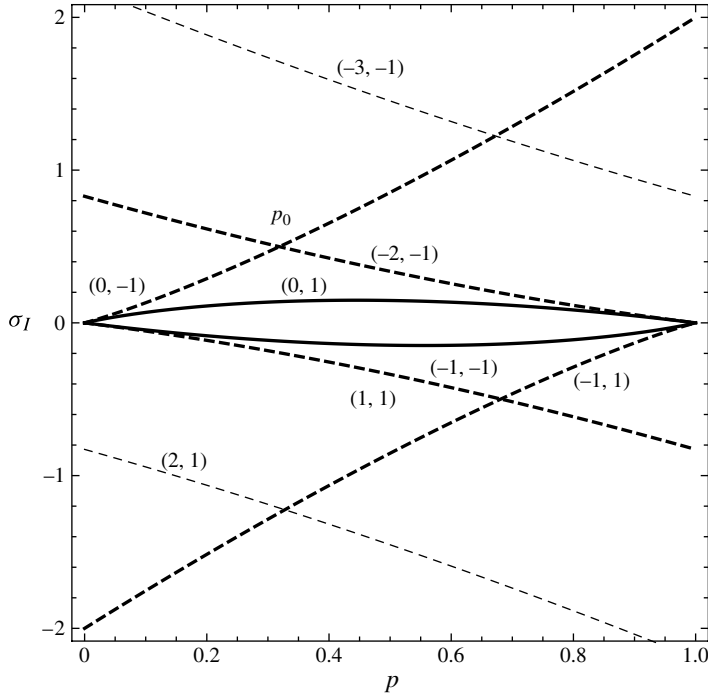


FIGURE 2. Imaginary part of eigenvalues at  $h = 0$  as a function of the wavenumber  $p$ . The continuous line marks the branches with negative Krein signatures whereas the dashed line corresponds to positive Krein signature. The value  $p_0 = 0.31875$  corresponds to the intersection between the branches  $(m, s) = (0, -1)$  and  $(-2, -1)$ .

$\mathbf{R}$  are identically zero. Apart from this eigenvalue pair, our computations (performed in double precision) revealed a pair of complex eigenvalues with magnitude  $10^{-8}$ . Since the condition numbers of the matrices  $\mathbf{L}$  and  $\mathbf{R}$  in (4.3) are large in this case and furthermore loss of accuracy is expected for close or multiple eigenvalues, we have also performed our computations in quadruple precision and further improved the accuracy in estimating this eigenvalue pair whose magnitude further reduced to  $10^{-16}$ .

## 5. Results

### 5.1. Superharmonic normal modes

In figure 3, we compare the imaginary part of eigenvalues for the superharmonic normal modes (as a function of non-dimensional wave height  $h$ ) with the results in Hogan (1988, his figure 1). In contrast to Hogan (1988), who reported instability of Crapper's waves for some amplitude ranges, our calculations reveal spectral stability to superharmonic disturbances for the entire range of amplitudes from zero to the maximum amplitude. Our results agree fairly well with those in Hogan (1988) for small amplitudes, including the collision between the two branches  $(m, s) = (-7, -1)$  and  $(4, -1)$  at  $h \approx 0.18$ . Note that the relationship between the wave steepness used in Hogan (1988) and  $h$  is  $ak = \pi h$ . As stated by the necessary condition for instability of MacKay & Saffman (1986), this collision does not result in loss of stability since the eigenvalues have the same signature (positive). On the other hand, Hogan (1988) suspected instability around this amplitude, since he thought mistakenly that the

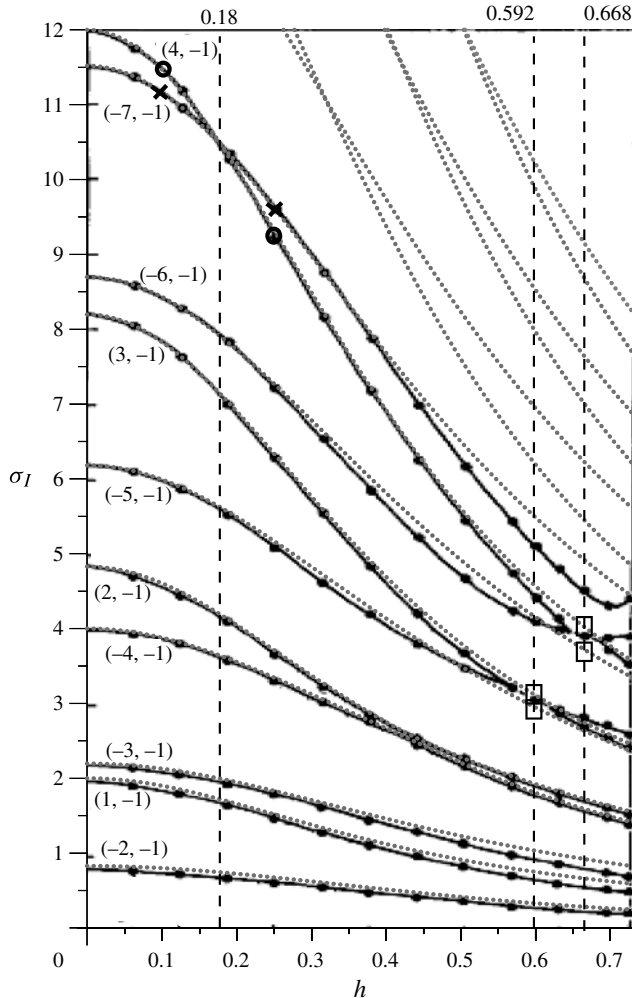


FIGURE 3. Imaginary part of the superharmonic normal modes as a function of non-dimensional amplitude  $h = H/\lambda$  ( $H$  is the wave height and  $\lambda$  is the wavelength): grey dotted lines, current results; black solid lines, results reported in Hogan (1988, his figure 1). On each branch, we mark the pair  $(m, s)$  corresponding to the spectrum at zero amplitude ( $h = 0$ ) given by (3.2).

colliding branches have opposite signatures. Our results show that the two branches in fact cross over each other following this collision without any sign of instability, as can be inferred from figure 4. In this figure, we can observe clearly where these branches reappear after the collision by examining eigenmodes for wave amplitudes bracketing the collision amplitude.

Furthermore, Hogan (1988) detected two pockets of instability for larger amplitudes: one centred around  $h = 0.592$  (see his figure 4) and the other centred around  $h = 0.668$  (see his figure 6). As shown in our figure 3, even though there are branches that approach each other at these amplitudes, no collision is detected from our computations using both double and quadruple precisions. Although it is not clear yet, we suspect that a probable cause of this discrepancy is the fact that Hogan

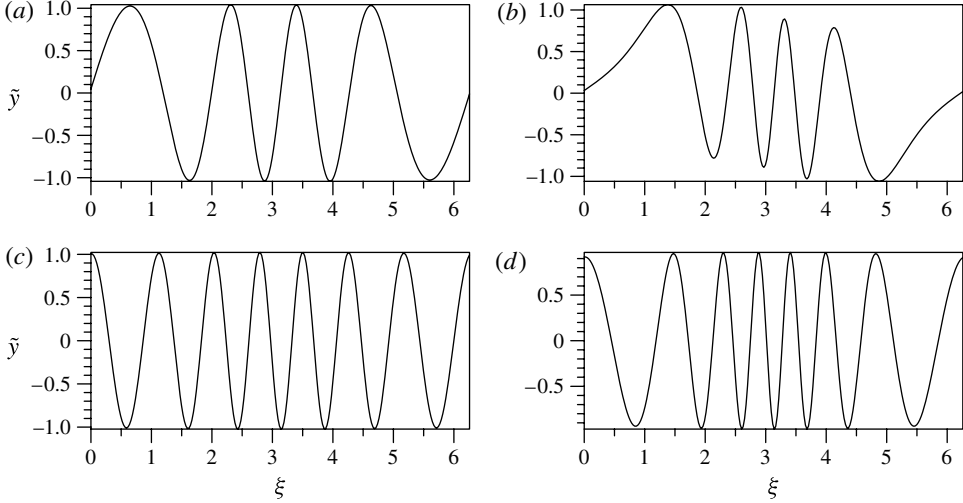


FIGURE 4. Four superharmonic normal modes corresponding to the two branches of  $(m, s) = (-7, -1)$  and  $(m, s) = (4, -1)$  that cross over at  $h \approx 0.18$ : (a,c) for  $h = 0.1$ ; and (b,d) for  $h = 0.2$ . We can infer that normal modes (a), with  $\sigma \approx 11.475 i$ , and (b), with  $\sigma \approx 9.32 i$ , marked with circles in figure 3, pertain to the branch  $(m, s) = (4, -1)$ ; whereas (c), with  $\sigma \approx 11.165 i$ , and (d), with  $\sigma \approx 9.6215 i$ , marked with crosses in figure 3, pertain to the branch  $(m, s) = (-7, -1)$ .

(1988) performed single-precision computations. As mentioned previously, Hogan (1988) justified the appearance of instability from collision of eigenvalues of different signature, but the signature of these eigenvalues is positive. Therefore, the necessary condition of MacKay (1986) is not fulfilled.

To validate our results, we integrate the exact evolution equations with an initial condition consisting of a superposition of the periodic wave solution and normal modes. The numerical method adopted here is a pseudospectral method for spatial discretization and a fourth-order Runge–Kutta scheme for time integration. We refer the reader to Li *et al.* (2004) for a detailed description. For the current simulations, we use 256 grid points (or, equivalently, 256 Fourier modes) within the  $2\pi$ -periodic domain and a time step of  $10^{-3}$ . We monitor conservation of mass, momentum and energy, and the magnitude of the relative error is of order  $10^{-14}$  within the time frame of the simulations.

We focus on the two amplitudes,  $h = 0.592$  and  $0.668$ , around which the two instability pockets were detected by Hogan (1988). For each of these amplitudes, we examine the time evolution of the two normal modes corresponding to the two branches that were predicted to collide by Hogan (1988). All these points are marked by squares in figure 3.

In figures 5 and 6, we depict the time evolution of the normal modes of  $(m, s) = (-5, -1)$  and  $(3, -1)$ , respectively, for  $h = 0.592$ . Based on our computations, they are neutrally stable with  $\sigma \approx 2.98301 i$  and  $\sigma \approx 3.1524 i$ . Our numerical solutions of the exact evolution equations show no sign of instability and compare well with the results from our linear stability analysis. Therefore, it can be concluded that our stability results for superharmonic perturbations are reliable. This conclusion is further confirmed by the comparison between our numerical solutions and our linear stability theory for  $h = 0.668$ , as shown in figures 7 and 8 corresponding to  $(m, s) = (-6, -1)$

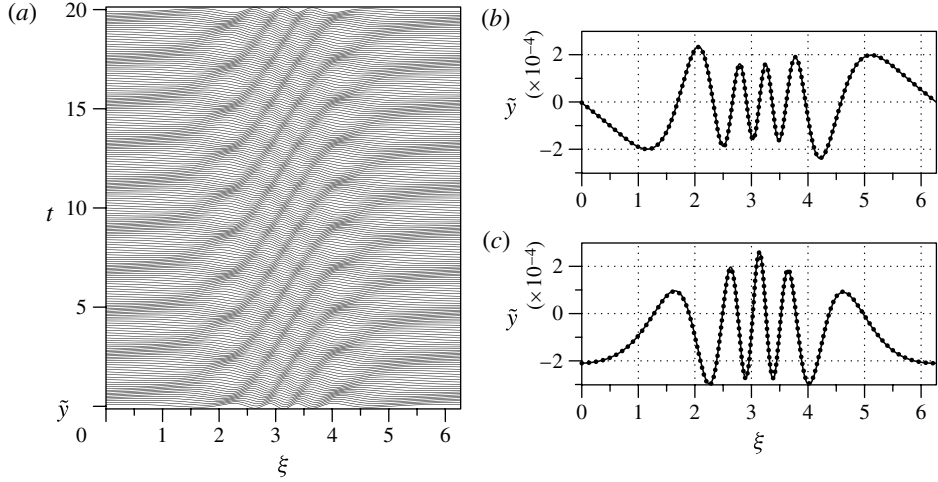


FIGURE 5. Time evolution of a superharmonic normal mode for  $(m, s) = (-5, -1)$  with  $\sigma = 2.98301 i$  for a periodic wave with amplitude  $h = 0.592$ . We present here the perturbation in  $y$  over one wavelength  $2\pi$ . (a) Numerical solution using the evolution code. (b,c) Comparison between the linear theory (dots) and the evolution code (solid lines) at  $t = 10$  and  $t = 20$ , respectively.

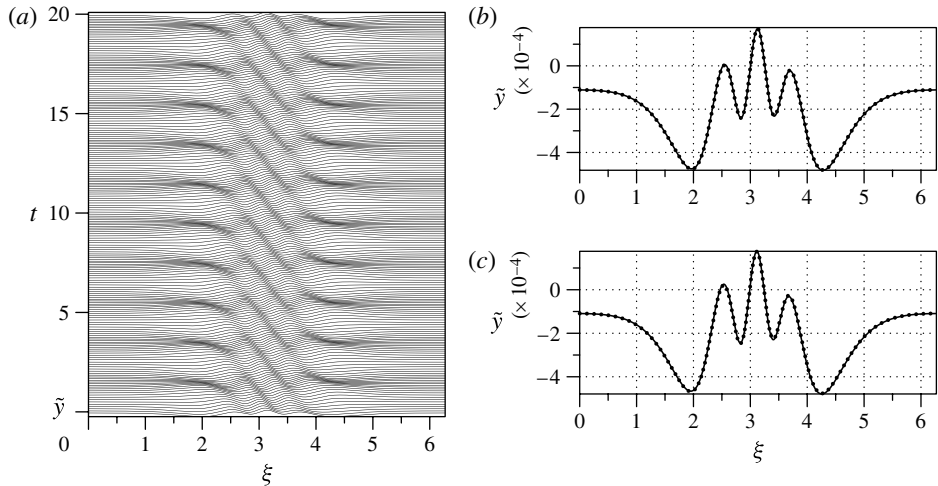


FIGURE 6. Same as figure 5 for  $h = 0.592$ , a superharmonic normal mode for  $(m, s) = (3, -1)$  with  $\sigma = 3.1524 i$ .

and  $(-7, -1)$ , respectively. These normal modes have eigenvalues of  $\sigma \approx 3.6974 i$  and  $\sigma \approx 3.9939 i$ , respectively, and are found to be neutrally stable, as our linear theory predicts.

### 5.2. Subharmonic instabilities

Our results indicate that Crapper's waves are unstable to subharmonic perturbations through collisions of eigenvalues of opposite signature, as evidenced in figure 9, where

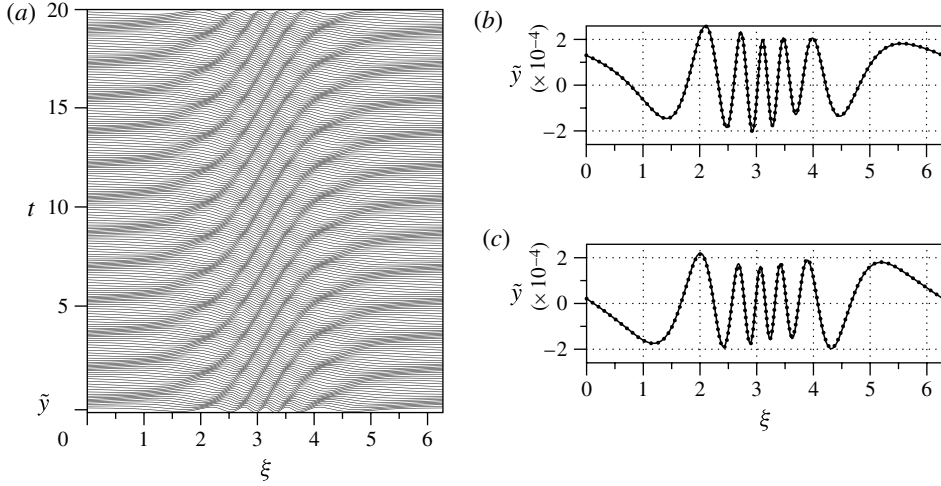


FIGURE 7. Same as figure 5 for  $h = 0.668$ , a superharmonic normal mode for  $(m, s) = (-6, -1)$  with  $\sigma = 3.6974 \text{ i}$ .

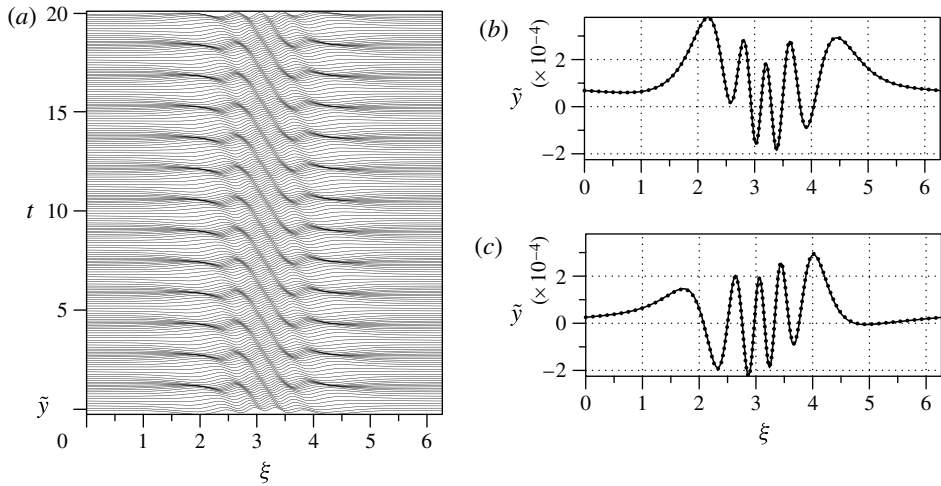


FIGURE 8. Same as figure 5 for  $h = 0.668$ , a superharmonic normal mode for  $(m, s) = (4, -1)$  with  $\sigma = 3.9939 \text{ i}$ .

the bifurcation diagrams for four different values of  $p$  are shown. This is consistent with the theory in MacKay & Saffman (1986). Note that, for each  $p$ , there are two pairs of eigenvalues of opposite signature at  $h = 0$  that collide eventually as the amplitude  $h$  becomes greater than certain critical values. Then two unstable modes, say,  $\sigma_1$  and  $\sigma_2$ , sprout. When  $p = 1/2$ , the two unstable modes become complex conjugate  $\sigma_1 = \sigma_2^*$  and thus satisfy the symmetry properties of the spectrum specified in § 2.4. As already conjectured in § 3 (see, in particular, figure 2), one collision occurs between the two branches of  $(m, s) = (1, 1)$  and  $(-1, -1)$ . The second collision occurs between  $(m, s) = (0, 1)$  and  $(0, -1)$  for  $p \in (0, 0.31875)$  while for  $p \in (0.31875, 0.5)$  between  $(m, s) = (0, 1)$  and  $(-2, -1)$ .

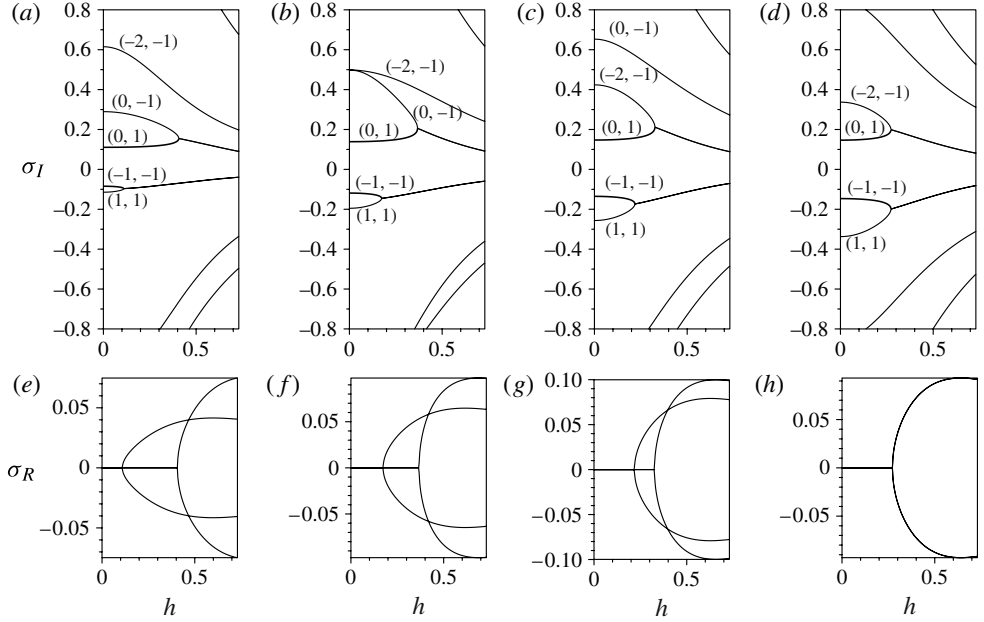


FIGURE 9. Bifurcation diagrams for subharmonic normal modes for (a,e)  $p = 0.2$ , (b,f)  $p = 0.31875$ , (c,g)  $p = 0.4$  and (d,h)  $p = 0.5$ . (a,b,c,d) Imaginary part of the normal modes as a function of non-dimensional amplitude  $h = H/\lambda$  ( $H$  is the wave height and  $\lambda$  is the wavelength). (e,f,g,h) Real part (growth rate). On each branch we mark the pair  $(m, s)$  corresponding to  $h = 0$  – see (3.2).

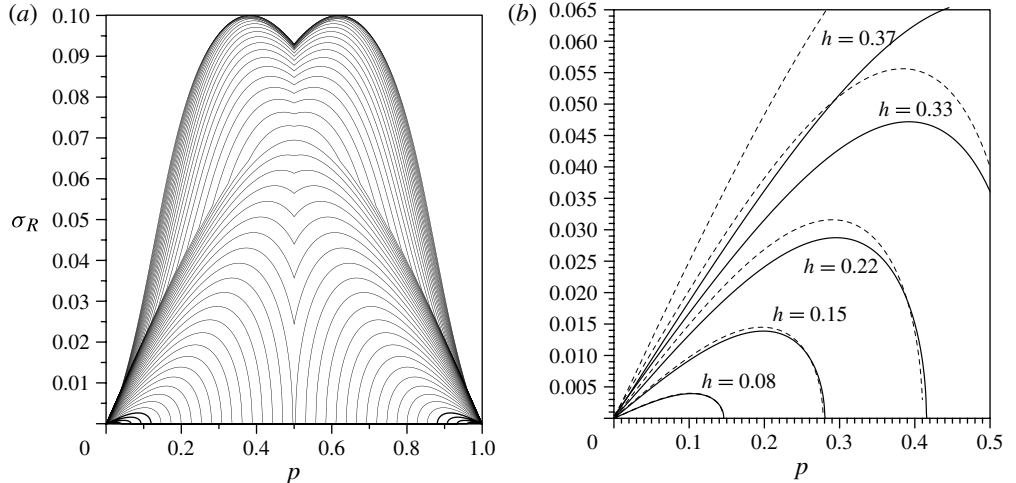


FIGURE 10. Subharmonic unstable modes. (a) The dependence of the growth rate (of the more unstable mode among the two shown in figure 9) on the perturbation wavenumber  $p$  for a series of equally spaced amplitudes in the range  $0 < h < 0.73$ . (b) Comparison to the weakly nonlinear theory (depicted here with dashed lines):  $\sigma_R = (p/8)\sqrt{3\pi^2 h^2 - 9p^2}$ .

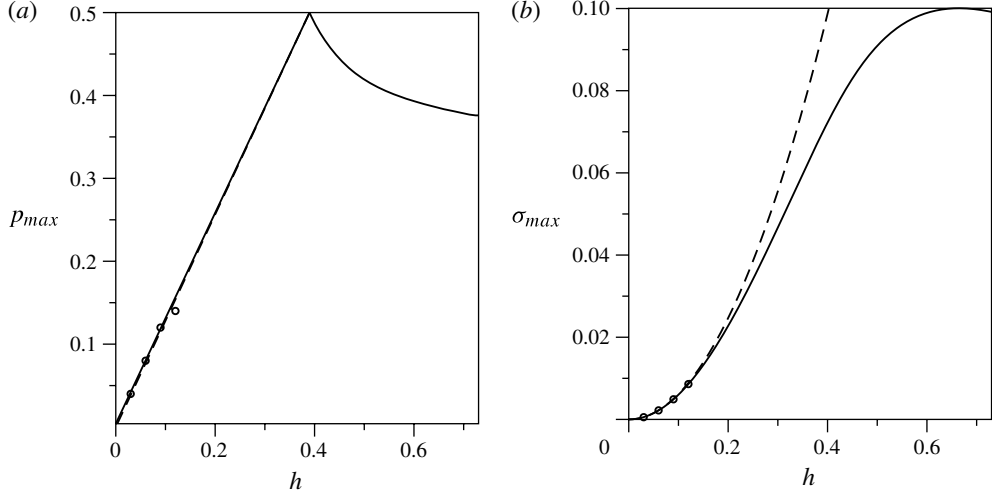


FIGURE 11. Subharmonic instability. (a) Wavenumber corresponding to the fastest-growing mode and (b) the corresponding growth rate. Continuous line, current theory; dashed line, weakly nonlinear theory ( $p_{max} = \pi h / \sqrt{6}$ ,  $\sigma_{max} = \pi^2 h^2 / 16$ ); circles, results in Chen & Saffman (1985).

Figure 10(a) shows the growth rate of the faster-growing mode (among the two depicted in figure 9) for a series of equally spaced amplitudes in the range of  $0 < h < 0.73$ . As shown in figure 10(b), our results for the growth rate compare well with the predictions of the weakly nonlinear theory based on the cubic nonlinear Schrödinger equation formulation (Chen & Saffman 1985) given by

$$\sigma_R = \frac{1}{8} (3\pi^2 h^2 p^2 - 9p^4)^{1/2}. \quad (5.1)$$

In figure 11, we show our results for the wavenumber of the most unstable mode and the corresponding growth rate. Note that both compare well with the numerical results of Chen & Saffman (1985) for  $0 < h < 0.12$ . In addition, in figure 11, the comparison with the weakly nonlinear theory given, from (5.1), by

$$p_{max} = \pi h / \sqrt{6} \quad \text{and} \quad \sigma_{max} = \pi^2 h^2 / 16 \quad (5.2)$$

is made and an excellent agreement is found even for wave amplitudes that we think are too large for the weakly nonlinear theory to be valid. Similar comparisons are made in figure 12 for the domain of instability in the  $(h, p)$  plane.

To conclude this section, we show a few comparisons between the numerical simulations of the exact evolution equations and the predictions of the linear theory. In the following, we consider a wave with amplitude close to the maximal ( $h = 0.7$ ) and subharmonic normal modes with  $p = 1/2$  (hence the spatial domain for the time evolution code contains two periods,  $4\pi$ ). The number of discretization points used is 512 while the time step is  $10^{-3}$ . In figure 13, we depict one of the two unstable normal modes for  $p = 1/2$ , whose eigenvalue is given by  $\sigma = 0.092 - 0.086i$ , while the other unstable eigenvalue is its complex conjugate, as a consequence of the symmetry properties of the spectrum discussed in § 2.4. The growth rate 0.092 is close to the maximal growth rate of, approximately, 0.1, which corresponds to a perturbation with wavenumber  $p \approx 0.36$ , as can be seen from figure 11(a). In figure 14, we show a

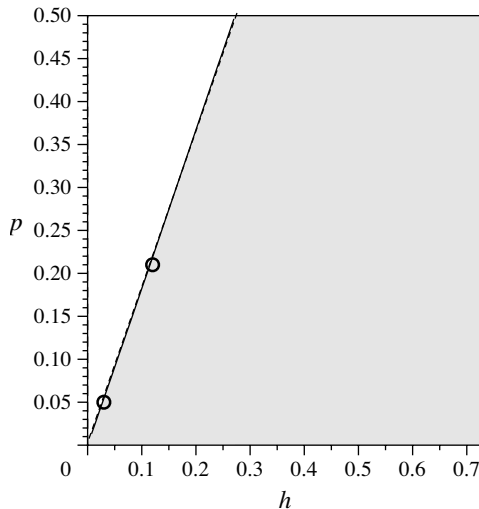


FIGURE 12. Domain of subharmonic instability in the  $(h, p)$  plane. Continuous line, current theory; dashed line, weakly nonlinear theory ( $p = \pi h/3$ ); circles, results in Chen & Saffman (1985).

neutral mode corresponding to the branch  $(m, s) = (-5, -1)$ , while one of the two decaying modes for  $p = 1/2$  (with  $\sigma = -0.092 - 0.086 i$ ) is shown in figure 15. Note that the agreement between the fully nonlinear simulations and the linear theory is good for all cases. It is interesting that the linear theory captures well the behaviour of the unstable normal mode even when its magnitude becomes so large that the linear theory is expected to break down, as evidenced by figure 13(c,d). We further remark that in figure 13(d) we have selected the time at which the surface profile touches itself. Beyond this particular time, the behaviour of the system can no longer be described by the model equations (2.1)–(2.6) since the topology of the fluid domain changes.

## 6. Concluding remarks

We have performed a linear stability analysis of Crapper's exact capillary wave solutions on deep water, investigating both superharmonic and subharmonic two-dimensional disturbances, for the entire range of amplitudes from zero to the maximum amplitude at which a trapped bubble is formed at the trough of the wave. To this end, as an alternative approach to the classical method of Longuet-Higgins (1978a,b), we have used a system of exact one-dimensional non-local evolution equations (Ovsjannikov 1974; Dyachenko *et al.* 1996), which yields a more compact formulation of the linear eigenvalue problem. In addition, we have solved the system numerically and compared our numerical solutions with the results from the linear stability analysis.

We have found that Crapper's capillary waves are linearly stable to superharmonic perturbations for the entire amplitude range. Our findings for superharmonic normal modes agree with Hogan's (1988) results for small amplitudes, but differ for larger amplitudes. We demonstrate the reliability of our results in this regime by comparing the time evolution of the normal modes with the direct numerical integration of the

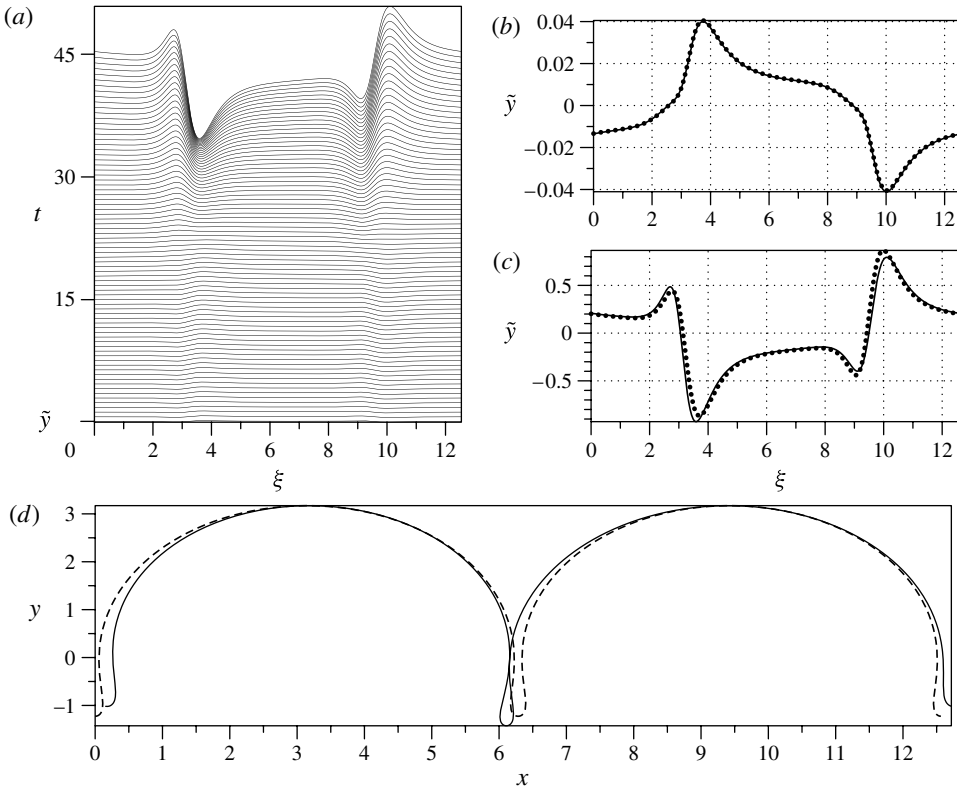


FIGURE 13. Time evolution of a subharmonic growing normal mode with  $p = 1/2$  and  $\sigma = 0.092 - 0.086 i$  for a periodic wave with amplitude  $h = 0.7$ . (We depict here the perturbation in  $y$  over two wavelengths  $4\pi$ .) (a) Numerical solution using the evolution code. (b,c) Comparison between the linear theory (dotted line) and evolution code (continuous line) at  $t = 20$  and  $t = 45.3$ , respectively. (d) Wave profile in the physical space at time  $t = 45.3$  (continuous line), and initial condition for the evolution code consisting of a wave of amplitude  $h = 0.7$  perturbed with the corresponding normal mode (dashed line).

exact evolution equations (using as initial condition a superposition of the solution of Crapper (1957) and the corresponding normal modes). The comparison between the predictions of the current theory and numerical simulations is excellent for all cases we have tested.

In the subharmonic regime, our work extends the previous study by Chen & Saffman (1985), whose results are limited to relatively small amplitudes. We find that Crapper's solution is unstable to subharmonic perturbations for the entire amplitude range. The wavenumber of the dominant instability increases almost linearly with the amplitude to  $p = 1/2$  in the range of  $0 \leq h \lesssim 0.4$  and then decreases monotonically to  $p \approx 1/3$  as  $h$  further increases. Our results for subharmonic perturbations agree for small amplitudes with both the results of Chen & Saffman (1985) and the predictions of the weakly nonlinear theory based on the cubic nonlinear Schrödinger equation. Comparisons with the direct numerical integration of the exact evolution equations is excellent, which demonstrates again the reliability of our analysis.

We remark, however, that viscous dissipation, which we have neglected, plays an important role in the propagation of periodic capillary waves and might subsequently

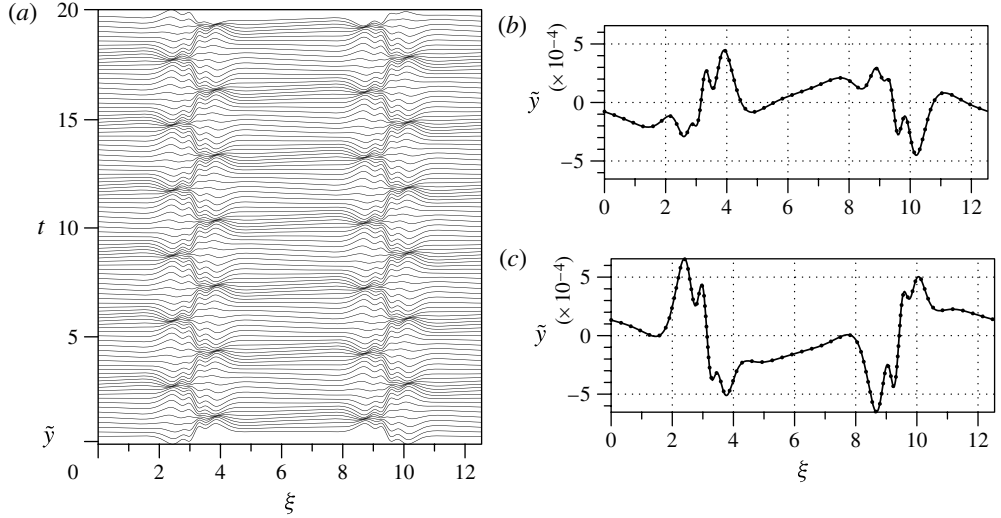


FIGURE 14. Time evolution of a subharmonic neutral normal mode with  $p = 1/2$  and  $\sigma = 2.001i$  (corresponding to the branch  $(-5, -1)$ ) for a periodic wave with amplitude  $h = 0.7$ . (We depict here the perturbation in  $y$  over two wavelengths  $4\pi$ .) (a) Numerical solution using the evolution code. (b,c) Comparison between the linear theory (dotted line) and evolution code (continuous line) at  $t = 10$  and  $t = 20$ , respectively.

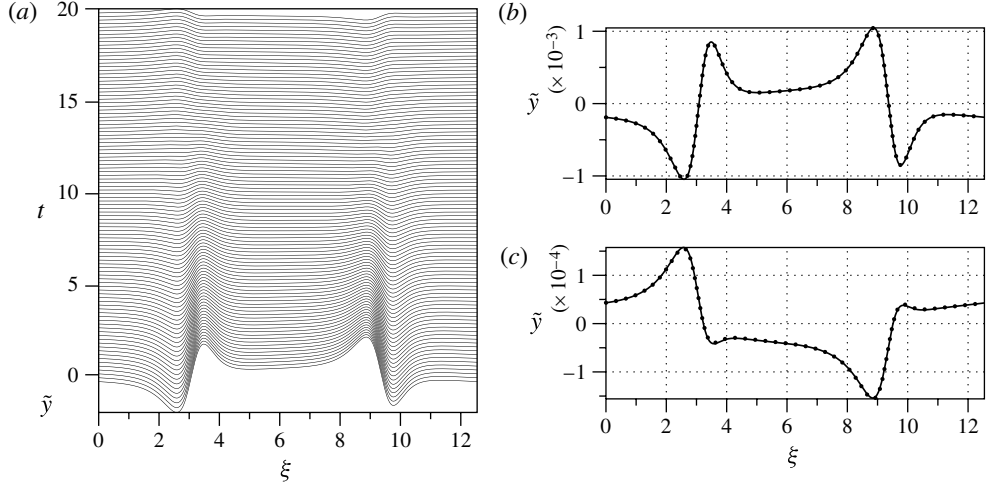


FIGURE 15. Same as figure 14, for a decaying normal mode with  $\sigma = -0.092 - 0.086i$ .

affect their instabilities. Lamb (1932) estimated the rate of decay of linear waves due to bulk viscosity as  $8\nu\pi^2/\lambda^2$ , where  $\nu$  is the kinematic viscosity ( $\approx 0.017 \text{ cm}^2 \text{ s}^{-1}$  for water) and  $\lambda$  is the wavelength (see Lamb 1932, Art. 348). This estimate has been confirmed experimentally by Davies & Vose (1965) for progressive wave trains of capillary waves with frequencies between 50 and 920 Hz (thus wavelengths ranging from approximatively 0.08 to 0.59 cm). Note that small-amplitude capillary waves of these wavelengths are expected to be dissipated by viscosity over 8–22 wave periods,

whereas the growth rate of dominant subharmonic instabilities predicted in this paper is approximately  $0.1/t_0$ , which corresponds to a time scale of 10 wave periods. Since the two time scales of growth and dissipation are comparable, it would be of interest and a challenge to confirm experimentally the result for finite-amplitude capillary waves presented in this paper.

We finally remark that it is straightforward to extend this work to capillary waves on fluid sheets of finite thickness, for which the exact solutions of Kinnersley (1976) are available. Thus, a two-dimensional analysis can be performed in a similar fashion by linearizing the non-local evolution equations for finite depth.

### Acknowledgements

The authors gratefully acknowledge support from the National Research Foundation of Korea funded by the Ministry of Education, Science, and Technology through the WCU program with grant no. R31-2008-000-10045-0.

### REFERENCES

- BENJAMIN, T. B. & FEIR, J. E. 1967 The disintegration of wave trains on deep water. *J. Fluid Mech.* **27**, 417–430.
- BENNEY, D. J. & ROSKES, G. J. 1969 Wave instabilities. *Stud. Appl. Maths* **48**, 377–385.
- CRAPPER, G. D. 1957 An exact solution for progressive capillary waves of arbitrary amplitudes. *J. Fluid Mech.* **2**, 532–540.
- CHEN, B. & SAFFMAN, P. G. 1985 Three-dimensional stability and bifurcation of capillary and gravity waves on deep water. *Stud. Appl. Maths* **72**, 125–147.
- CHOI, W. & CAMASSA, R. 1999 Exact evolution equations for surface waves. *J. Engng Mech.* **125**, 756–760.
- DAVIES, J. T. & VOSE, R. W. 1965 On the damping of capillary waves by surface films. *Proc. R. Soc. Lond. A* **286**, 218–234.
- DECONINCK, B. & OLIVERAS, K. 2011 The instability of periodic surface gravity waves. *J. Fluid Mech.* **675**, 141–167.
- DIAS, F. & KHARIF, C. 1999 Nonlinear gravity and capillary–gravity waves. *Annu. Rev. Fluid Mech.* **31**, 301–346.
- DJORDJEVIC, V. D. & REDEKOPP, L. G. 1977 On two-dimensional packets of capillary–gravity waves. *J. Fluid Mech.* **79**, 703–714.
- DYACHENKO, A. L., ZAKHAROV, V. E. & KUZNETSOV, E. A. 1996 Analytical description of the free surface dynamics of an ideal fluid (canonical formalism and conformal mapping). *Phys. Lett. A* **221**, 73–79.
- GARBOW, B. S. 1978 Algorithm 535: the QZ algorithm to solve the generalized eigenvalue problem for complex matrices [F2]. *ACM Trans. Math. Softw.* **4** (4), 404.
- HAMMACK, J. L. & HENDERSON, D. M. 1993 Resonant interactions among surface water waves. *Annu. Rev. Fluid Mech.* **25**, 55–97.
- HOGAN, S. J. 1985 The fourth-order evolution equation for deep-water gravity–capillary waves. *Proc. R. Soc. Lond. A* **402**, 359–372.
- HOGAN, S. J. 1988 The superharmonic normal mode instabilities of nonlinear deep-water capillary waves. *J. Fluid Mech.* **190**, 165–177.
- KINNERSLEY, W. 1976 Exact large amplitude waves on sheets of fluid. *J. Fluid Mech.* **77**, 229–241.
- LAMB, H. 1932 *Hydrodynamics*, 6th edn. Cambridge University Press.
- LI, Y. A., HYMAN, J. M. & CHOI, W. 2004 A numerical study of the exact evolution equations for surface waves in water of finite depth. *Stud. Appl. Maths* **113**, 303–324.
- LONGUET-HIGGINS, M. S. 1978a The instabilities of gravity waves of finite amplitude in deep water. I. Superharmonics. *Proc. R. Soc. Lond. A* **360**, 471–488.

- LONGUET-HIGGINS, M. S. 1978*b* The instabilities of gravity waves of finite amplitude in deep water. II. Subharmonics. *Proc. R. Soc. Lond. A* **360**, 489–505.
- MACKAY, R. S. 1986 Stability of equilibria of Hamiltonian systems. In *Nonlinear Phenomena and Chaos* (ed. S. Sarkar). Adam Hilger.
- MACKAY, R. S. & SAFFMAN, P. G. 1986 Stability of water waves. *Proc. R. Soc. Lond. A* **406**, 115–125.
- MCLEAN, J. W. 1982*a* Instabilities of finite-amplitude water waves. *J. Fluid Mech.* **114**, 315–330.
- MCLEAN, J. W. 1982*b* Instabilities of finite-amplitude gravity waves on water of finite depth. *J. Fluid Mech.* **114**, 331–341.
- MCLEAN, J. W., MA, Y. C., MARTIN, D. U., SAFFMANN, P. G. & YUEN, H. C. 1981 Three dimensional instability of finite-amplitude water waves. *Phys. Rev. Lett.* **46**, 817–821.
- NICHOLLS, D. P. 2009 Spectral data for travelling water waves: singularities and stability. *J. Fluid Mech.* **624**, 339–360.
- OVSJANNIKOV, S. J. 1974 To the shallow water theory foundation. *Arch. Mech.* **26**, 407–422.
- SWARZTRAUBER, P. N. 1982 Vectorizing the FFTs. In *Parallel Computations* (ed. G. Rodrigue), pp. 51–83. Academic.
- VANDEN-BROECK, J.-M. & KELLER, J. B. 1980 A new family of capillary waves. *J. Fluid Mech.* **98**, 161–169.
- ZAKHAROV, V. E. 1968 Stability of periodic waves of finite amplitude on the surface of a deep fluid. *J. Appl. Mech. Tech. Phys.* **2**, 190–194.
- ZHANG, J. & MELVILLE, W. K. 1987 Three-dimensional instabilities of nonlinear gravity–capillary waves. *J. Fluid Mech.* **174**, 187–208.